

Exclusive Production of Higgs Bosons in Hadron Colliders *

Hung Jung Lu and Joseph Milana

Department of Physics, University of Maryland

College Park, Maryland 20742

(June 12, 2021)

Abstract

We study the exclusive, double-diffractive production of the Standard Model Higgs particle in hadronic collisions at LHC and FNAL (upgraded) energies. Such a mechanism would provide an exceptionally clean signal for experimental detection in which the usual penalty for triggering on the rare decays of the Higgs could be avoided. In addition, because of the color singlet nature of the hard interaction, factorization is expected to be preserved, allowing the cross-section to be related to similar hard-diffractive events at HERA. Starting from a Fock state expansion in perturbative QCD, we obtain an estimate for the cross section in terms of the gluon structure functions squared of the colliding hadrons. Unfortunately, our estimates yield a production rate well below what is likely to be experimentally feasible.

12.15.Ji, 12.38.Bx, 13.85.-t, 14.80.Gt

Typeset using REVTeX

*Work supported by the Department of Energy, contract DE-FG02-93ER-40762.

I. INTRODUCTION

The field of hard diffractive scattering has acquired a solid experimental basis with the report last year [1] of the UA8 data observing jet events in conjunction with an elastically scattered hadron at the $Spp\bar{p}S$ collider at CERN. Similar findings [2] by ZEUS of large rapidity gap, jet events at HERA are also suggestive of such diffractive events, although the existence of a final state proton still needs to be confirmed. One interesting application of such diffractive events would be in the search for fundamental new physics, Higgs bosons. Such possibilities have indeed been discussed before [3–6], although mostly in the context of inclusive, diffractive processes:

$$p + p \rightarrow H + p + p + X. \quad (1.1)$$

Here we are interested on the other hand with the truly exclusive, double–diffractive production:

$$p + p \rightarrow H + p + p. \quad (1.2)$$

This interest is two fold. First, because the experimental signal for this process would be exceptionally clean with the final state hadrons well separated in rapidity from the Higgs decay fragments, it should be possible to trigger on the dominant decays of the Higgs particle, ($b\bar{b}$ jet-pairs for $m_H < .8$ TeV) rather than on a rare decay mode as is necessary in the case of inclusive Higgs production [7,8] due to the otherwise unmanageable backgrounds. To the extent that (1.2) does occur, one would expect, due to the narrow width of a Standard–Model Higgs (for instance, $\Gamma(H \rightarrow all) \approx \Gamma(h \rightarrow b\bar{b}) = 2.5$ MeV for $m_H = 100$ GeV), that it would stand out rather prominently above the corresponding background of double–diffractive $b\bar{b}$ jet-pairs. The use of the silicon–vertex technology by which CDF [9] is now exploiting to tag top decays into bottom quarks should particularly help suppress the background, eliminating the analogous jet events of light parton ($gg, u\bar{u}, d\bar{d}$, etc.) pairs.

Secondly, it is our expectation that events such as (1.2) (and their background) should obey factorization. In comparison, estimates for inclusive production of the Higgs [3–5] are

likely to be less reliable due to the expected breakdown of factorization. These expectations are based upon the observation of Collins, Frankfurt, and Strikman [10] (see also Ref. [11] in this regard) that in the case that a hard scattering event produces a color octet state, it is impossible to disentangle the soft and hard physics processes involved in diffractive events. In more technical terms, the limitation in the final state to an elastically scattered hadron prevents the sum over all possible cuts of the hard scattering graphs necessary to eliminate soft gluon exchanges in the proofs of factorization [12] for inclusive processes. These authors then predict that in the case of “coherent diffractive events”, where all the momentum lost by the proton appears in the hard scattering event, factorization should be violated at the leading twist level, showing up most dramatically in dijet diffractive events at HERA in which such “coherent” events would be higher-twist relative to the “incoherent” diffractive events due to the color-singlet nature of the hard interaction. While agreeing with these general arguments we pointed out in Ref. [13] that some of these predictions may nevertheless not be so obvious due to the potential complications in these rates of an additional expansion in $1/\xi$, the energy loss of the diffracted proton. (Depending upon the low energy behavior of the soft physics, the higher-twist suppression might be compensated at least in part, by differing powers in $1/\xi$ between the “coherent” vs. “incoherent” mechanisms.) Irrespective though of these complications, in the present case we do not believe the considerations of [10] should apply as the hard scattering event now involves a color singlet process, and hence, although in itself higher-twist, additional soft gluon exchanges should be suppressed. Indeed we believe all such exclusive double-diffracted, jet events should be added to the otherwise exhaustive list of experimental processes in Ref. [14] for exploring the nature of hard diffractive scattering.

In Ref. [4] an estimate of the cross section for Higgs production via exclusive double diffraction in a Pomeron based model was obtained, with a value $\sigma \sim 10^{-6}$ pb for a Higgs mass of 150 GeV. Although this is a small cross section, nonetheless it might be accessible for measurement given the uncertainty in the theoretical prediction or an improvement in experimental luminosity. Indeed at the planned luminosities of the LHC ($\mathcal{L} = 1.7 \times$

$10^{34} (\text{cm}^{-2} - \text{sec}^{-1})$ [15]), such a rate could correspond to a half-dozen or so events per year at these Higgs masses, depending upon the overall coefficient assignable to this order of magnitude estimate. This in itself is competitive with the present status of top quark events being searched for at FNAL [9,16]. On the other hand, due to the steep dependence with Higgs mass of the rate for (1.2), significantly more abundant yields (hundreds) would be anticipated if the mass of the Higgs was at the lower end of the presently allowable values ($m_H > 64 \text{ GeV}$ [17]) assuming the estimates of [4] were correct. Given the cleanness of the signal for the Higgs boson, it is important to further explore this mechanism. In particular, it is highly desirable to have an alternative and independent estimate of the production cross section.

Note that we will not consider here Higgs production through photon-photon fusion. This mechanism, considered elsewhere [18] (although predominantly in the context of nuclear-nuclear collisions and for collider parameters more ambitious than being presently projected [15]) also produces the desired double-diffracted signature. However it involves coherent radiation of photons off of the entire hadron and hence are not amenable to a partonic type analysis to be employed here. All results should therefore be understood to apply to these latter (“Pomeron-Pomeron” fusion) type of mechanisms.

In a previous paper [13], we employed a Fock state expansion in perturbative QCD to compute hard-diffractive events in electron-proton collisions. We showed that in this approach, and consistent with other estimates in related processes [19,20], the unknown soft matrix element that entered the amplitude for these events at HERA can be related to the gluon structure function in the low- x region. In this paper we apply this method to the exclusive production of Higgs bosons at hadron-hadron colliders. In addition to the generic triangle loop diagram considered in Refs. [3-6], we have included in our analysis the creation of the Higgs particle through box and pentagon top-quark loops. Indeed in our approach these contribute roughly equally in the amplitude for the process being considered and to our best knowledge, have not been considered previously.

Unfortunately our estimates yield that the cross section at either upgraded Fermilab

(FNAL*) energies or at the LHC is particularly small and hence, despite the potential cleanness of the signal, we do not expect the double-diffractive mechanism to be useful at either laboratory for discovering the Higgs boson.

II. EFFECTIVE HIGGS-GLUON INTERACTION

As we will argue in the next section, the dominant contribution to the exclusive production of Higgs comes from processes involving gluons in the initial and final state. Hence we will need to know the interaction between gluons and Higgs. In particular, we will need the effective interaction vertices of two, three and four gluons with a Higgs particle.

The Higgs particle does not couple directly to gluons. However, it can do so through a quark loop. Since the Yukawa coupling of the Higgs particle is proportional to the mass of the coupled fermion, we need only to consider the top-quark loop. The effects of lighter quarks (u, d, s, c, b) are negligible due to the substantially heavier mass of the top quark. We will consider the regime $m_H \leq m_t$, where m_H is the Higgs mass and m_t the top mass. As we will see later, the Higgs production cross section decreases with increasing Higgs mass. Therefore, the $m_H \leq m_t$ regime is where one can expect a higher cross section. The restriction to the case of lighter Higgs masses has the technical benefit that it significantly facilitates the computation of the Feynman integrals since we can compute all integrals to leading order in m_H/m_t . The expansion in m_H/m_t is better in fact than one might naively expect, as the relevant parameter is the ratio of the two masses multiplied by a typical value of one or more Feynman parameters entering the particular loop's evaluation, so that even at $m_H/m_t \approx 1$, corrections are small (see Ref. [21] for explicit calculations of the higher corrections to this approximation in the case of inclusive Higgs production). Indeed, the more Feynman parameters (heavy quark propagators) the better the approximation.

In this limit, the heavy top-quark loop integrates out and the Higgs particle becomes effectively coupled to the gluons. In Fig. 1 we present the effective interaction vertices $ggH, gggH, ggggH$ between the Higgs particle and gluons. Notice in particular the momen-

tum flow convention for the ggH and $gggH$ vertices. In the figure, a, b, c, d represent the color indices and $\lambda, \mu, \nu, \sigma$ the Lorentz indices of the external gluons.

The following are the analytical results for the interaction vertices, where g_w and g_s are the weak $SU(2)$ and the strong $SU(3)$ coupling constant, and m_W the mass of the W gauge boson.

$$iG_{\lambda\mu}^{ab}(k_1, k_2) = \frac{i}{24\pi^2} \frac{g_w g_s^2}{m_W} \delta^{ab} (g_{\lambda\mu} k_1 k_2 - k_{2\lambda} k_{1\mu}), \quad (2.1)$$

$$iG_{\lambda\mu\nu}^{abc}(k_1, k_2, k_3) = \frac{1}{24\pi^2} \frac{g_w g_s^3}{m_W} f^{abc} [g_{\lambda\mu} (k_1 - k_2)_\nu + g_{\mu\nu} (k_2 - k_3)_\lambda + g_{\nu\lambda} (k_3 - k_1)_\mu], \quad (2.2)$$

$$\begin{aligned} iG_{\lambda\mu\nu\sigma}^{abcd}(k_1, k_2, k_3, k_4) = & \frac{i}{24\pi^2} \frac{g_w g_s^4}{m_W} [f^{abe} f^{cde} (g_{\lambda\nu} g_{\mu\sigma} - g_{\lambda\sigma} g_{\mu\nu}) \\ & + f^{ace} f^{bde} (g_{\lambda\mu} g_{\nu\sigma} - g_{\lambda\sigma} g_{\mu\nu}) \\ & + f^{ade} f^{bce} (g_{\lambda\mu} g_{\nu\sigma} - g_{\lambda\nu} g_{\mu\sigma})]. \end{aligned} \quad (2.3)$$

Notice the ggH vertex satisfy the conditions

$$k_1^\lambda iG_{\lambda\mu}^{ab}(k_1, k_2) = 0 = iG_{\lambda\mu}^{ab}(k_1, k_2) k_2^\mu. \quad (2.4)$$

The expression for the triangle diagram Eq. (2.1) has been known for sometime [22]. Note the similarity between the $gggH$ and $ggggH$ vertices with the conventional form of the pure-QCD three- and four-gluon vertices. Observe, however, that the three momenta k_1, k_2, k_3 in the $gggH$ vertex are independent variables, as opposed to the case of the pure-QCD three-gluon vertex. Observe also that the expression for the $ggggH$ vertex does not contain an explicit dependence on the external momenta, just like in the case of the pure-QCD four-gluon vertex. Finally, notice that the effective gluon-Higgs vertices do not depend on the value of the top-quark mass (this is valid only for the $m_H \leq m_t$ regime.)

III. SCATTERING AMPLITUDE

The leading diagram for the exclusive production of Higgs bosons is depicted in Fig. 2. This figure can be interpreted as the production of a Higgs particle through pomeron-pomeron fusion, where the two gluon lines belonging to the same proton effectively represent

the pomeron interaction. In principle the partons coming out of the protons could also be quarks, in which case Higgs production would occur through two possible mechanisms: 1) fusion of virtual $Z^0 Z^0$ pairs radiated off of diffracted quarks, or 2) $q\bar{q}$ fusion with an additional hard gluon pair creating the same flavor quarks back into the colliding hadrons. In our previous work [13] on exclusive dijet diffractive production at HERA, such quark initiated contributions were suppressed due to an anticipated less singular behavior in the small- x region of the soft matrix elements entering the hard amplitude, occurring because of a partial cancellation between quark and antiquark graphs. This thus lead us to approximate the soft matrix elements by the valence quark distribution functions. In the present case such a cancellation only occurs in the case of Z^0 particle fusion, for which we estimate a suppression in the amplitude of the order of 10^{-2} arising (as we will see below) from the ratio of valence quark to gluon structure functions squared. In the case of $q\bar{q}$ fusion, due to the explicit mass dependence of the coupling of quarks to the Higgs, these graphs will also be suppressed either directly through the vanishingly small couplings ($m_u \approx m_d \approx m_s \approx m_c \approx 0$) or because of the highly suppressed probabilities of finding bottom quarks (relative to gluons) in a proton.

Having now argued why only the gluon initiated processes need be considered, we proceed with our evaluation of Fig. 2 using perturbative QCD methods. Many of the steps in our approach were already detailed in Ref. [13]; we repeat them here for the sake of completeness. In the Fock component expansion [23,24], a proton can be expressed in terms of its parton (quark and gluon) components as

$$|p\rangle = \sum_n \int [dx][d^2k_\perp] \frac{1}{\sqrt{x_1 \cdots x_n}} \psi_n(x_i, k_{i\perp}) |x_i, k_{i\perp}\rangle, \quad (3.1)$$

where x_i are the longitudinal momentum fraction of the proton carried by the i -th component parton and $k_{i\perp}$ the corresponding transverse momentum. We have suppressed color and spin indices here. The individual parton states are normalized by

$$\langle p'_i | p_j \rangle = 16\pi^3 x_i \delta(x'_i - x_j) \delta^{(2)}(k'_{i\perp} - k_{j\perp}) \quad (3.2)$$

and the measure is defined by

$$[dx][d^2k_\perp] = \left(\prod_{i=1}^n dx_i \frac{d^2k_{i\perp}}{16\pi^3} \right) \delta\left(1 - \sum_{j=1}^n x_j\right) 16\pi^3 \delta^{(2)}\left(\sum_{j=1}^n k_{j\perp}\right). \quad (3.3)$$

The wavefunctions obey the constraint

$$1 = \sum_n \int [dx][d^2k_\perp] |\psi_n(x_i, k_{i\perp})|^2, \quad (3.4)$$

so that one obtains the canonical normalization for the proton that

$$\langle p | p' \rangle = 16\pi^3 E \delta^3(p - p'). \quad (3.5)$$

Let ξ_1 be the fraction of momentum loss of the first hadron and ξ_2 the corresponding fraction of momentum loss of the second hadron. We thus have for Fig. 2

$$p'_1 = (1 - \xi_1)p_1, \quad (3.6)$$

$$p'_2 = (1 - \xi_2)p_2. \quad (3.7)$$

In Fig. 3 we show the Feynman diagrams for the hard matrix element involving four external gluons and one Higgs particle. Fig. 3a, 3b, 3c represent typical Feynman diagrams for the s -channel, u -channel and the four-gluon-vertex exchange mechanisms. As discussed in the previous section, the effective gluon-Higgs coupling vertices are induced by a heavy top-quark loop. The Higgs line can be attached to any gluon line, three-gluon vertex or four-gluon vertex. Hence, we have 7 diagrams for the s - or u -channel exchange mechanism, and 5 diagrams for the four-gluon-vertex exchange. The effective ggH , $gggH$, $ggggH$ vertices are given in Eq. (2.1), (2.2) and (2.3).

At the parton level, we define x_1 to be the fraction of momentum of hadron one, p_1 , carried by the first incoming gluon and x'_1 the fraction of momentum of the diffracted hadron one, p'_1 , carried by the first outgoing gluon. The momentum fractions x_1 and x'_1 are related by

$$x_1 = \xi_1 + x'_1(1 - \xi_1). \quad (3.8)$$

Similarly, we define y_1 and y'_1 to be the corresponding initial and final momentum fractions of the gluon from the second hadron. These momentum fractions are related by

$$y_1 = \xi_2 + y'_1(1 - \xi_2). \quad (3.9)$$

The kinematics of hard diffraction considerably simplifies the calculation. In particular, the gluon polarization vectors are orthogonal to the four-momenta of all the incoming and outgoing gluons, hence a large number of dot products vanish.

Defining $\tilde{x}_1 = (1 - \xi_1)x'_1$ and $\tilde{y}_1 = (1 - \xi_2)y'_1$, averaging over initial helicity and color, and considering only the case of final gluons that conserve the initial color and helicity, the scattering amplitude from the s -channel contribution (or u -channel contribution, which turns out to be identical) is given by

$$i\mathcal{M}^{(s,u)} = \frac{i}{16} \frac{g_w \alpha_s^2}{m_W} \left[-2 + \frac{x_1}{\tilde{x}_1} + \frac{\tilde{x}_1}{x_1} + \frac{y_1}{\tilde{y}_1} + \frac{\tilde{y}_1}{y_1} - \frac{2x_1 y_1}{\tilde{x}_1 \tilde{y}_1} - \frac{2\tilde{x}_1 \tilde{y}_1}{x_1 y_1} \right], \quad (3.10)$$

where g_w is the $SU(2)$ weak coupling constant and is related to the Fermi constant by $G_F/\sqrt{2} = g_w^2/8m_W^2$ (to tree level), with m_W the mass of the W boson. And α_s is the strong coupling constant. Analogously, the total contribution from the four-gluon-vertex diagrams, averaged over initial helicities and colors, is given by

$$i\mathcal{M}^{(4g)} = \frac{i}{8} \frac{g_w \alpha_s^2}{m_W} \left[2 - \frac{x_1}{\tilde{x}_1} - \frac{\tilde{x}_1}{x_1} - \frac{y_1}{\tilde{y}_1} - \frac{\tilde{y}_1}{y_1} \right]. \quad (3.11)$$

The total hard amplitude is simply the sum of the s -channel, u -channel and the four-gluon-vertex contributions:

$$i\mathcal{M}^{\text{hard}} = i\mathcal{M}^{(s)} + i\mathcal{M}^{(u)} + i\mathcal{M}^{(4g)} = -\frac{i}{4} \frac{g_w \alpha_s^2}{m_W} \left[\frac{x_1 y_1}{\tilde{x}_1 \tilde{y}_1} + \frac{\tilde{x}_1 \tilde{y}_1}{x_1 y_1} \right]. \quad (3.12)$$

To obtain the scattering amplitude of $p + p \rightarrow p + p + H$ at the hadronic level, we must sandwich the hard amplitude between the bras and kets of the incoming and outgoing hadrons. Using Eq. (3.1–3.3),

$$\begin{aligned} i\mathcal{M} &= \langle p'_1 p'_2 | i\mathcal{M}^{\text{hard}} | p_1 p_2 \rangle \\ &= \sum_n (1 - \xi_1)^{(n-1)/2} \int \frac{[dx'] [d^2 k'_\perp]}{\sqrt{x'_1 x_1}} \psi_n^*(x', k'_\perp) \psi_n(x, k'_\perp) \\ &\quad \sum_m (1 - \xi_2)^{(m-1)/2} \int \frac{[dy'] [d^2 q'_\perp]}{\sqrt{y'_1 y_1}} \psi_m^*(y', q'_\perp) \psi_m(y, q'_\perp) i\mathcal{M}^{\text{hard}}, \end{aligned} \quad (3.13)$$

in which the parton momenta are related by Eq. (3.8), (3.9) and

$$x_i = (1 - \xi_1)x'_i, \quad y_i = (1 - \xi_2)y'_i, \quad i = 2 \cdots n. \quad (3.14)$$

These soft-matrix elements are precisely those found in our previous work [13] on dijet diffractive events at HERA.

As in [13], in order to continue we need to introduce approximations and estimate the soft matrix elements contained in the previous equation. Guided by the ‘handbag’ appearance of the amplitude in Fig. 2, we note in the case of the helicity conserving amplitudes the resemblance of the soft matrix elements to the gluon’s structure function [24,25]:

$$G_{g/p}(x_1) = \sum_n \sum_a \int [dx][d^2k_\perp] |\psi_n(x, k_\perp)|^2 \delta(x_a - x_1). \quad (3.15)$$

The second sum is over all gluons in a given Fock component. For the case at hand that $\xi \ll 1$, we note from Eq. (3.14) that $x'_i \approx x_i$ for all $i = 2 \cdots n$, and for $x'_1 > \xi_1$. And similarly $y'_i \approx y_i$ for all $i = 2 \cdots n$, and for $y'_1 > \xi_2$. We also make the approximation $\tilde{x}_1 \approx x_1$ and $\tilde{y}_1 \approx y_1$. For the helicity conserving processes,¹ we therefore estimate Eq. (3.13) by

$$i\mathcal{M} = \int_{\xi_1}^1 \frac{dx}{x} G_{g/p}(x) \int_{\xi_2}^1 \frac{dy}{y} G_{g/p}(y) i\mathcal{M}^{\text{hard}}, \quad (3.16)$$

where in our approximation, the hard amplitude is given by

$$i\mathcal{M}^{\text{hard}} = -\frac{i g_w \alpha_s^2}{2 m_W}. \quad (3.17)$$

IV. HIGGS PRODUCTION CROSS SECTION

The expression for the cross section of the $p + p \rightarrow p + p + H$ process is given by

¹As in [13], we assume that the gluon structure function is quantitatively the largest soft-matrix element so that helicity flipping events (in which the polarizations of the gluons leaving and re-entering the proton are opposite) are taken to be suppressed.

$$d\sigma = \frac{|\mathcal{M}|^2}{2^8\pi^3s} \delta(\xi_1\xi_2s - m_H^2) d\xi_1 dt_1 d\xi_2 dt_2, \quad (4.1)$$

where $t_1 = (p_1 - p'_1)^2$, $t_2 = (p_2 - p'_2)^2$, and m_H^2 is the mass of the Higgs particle. In the calculation of the hard amplitudes we have used the diffractive limit ($t_1, t_2 \rightarrow 0$). For the integration of t_1 and t_2 away from the diffractive limit we include in Eq. (4.1) the form factors e^{bt_1} and e^{bt_2} , and use $b \sim 4 \text{ GeV}^{-2}$ (see Ref. [13,26].) In our approach these form factors represent a modeling of the allowable (i.e. “intrinsic”) transverse momentum dependence of the active partons. After integrating out these variables, we obtain for the total cross section

$$\sigma = \frac{1}{256\pi^2} \frac{\alpha_w \alpha_s^4}{s^2 m_W^2 b^2} \int_{m_H^2/s}^1 \frac{d\xi}{\xi} \left[\int_{\xi}^1 \frac{dx}{x} G_{g/p}(x) \right]^2 \left[\int_{m_H^2/\xi s}^1 \frac{dy}{y} G_{g/p}(y) \right]^2. \quad (4.2)$$

In order to simplify the above integrals, we use the following parametrization for the gluon structure function:²

$$G_{g/p}(x, Q^2 = M_H^2) = \frac{c(1-x)^5}{x^{3/2}}. \quad (4.3)$$

This low- x singular form is in general agreement with both theoretical expectations [27,28] at these Q^2 values, and also the most recent data from HERA [29,30]. We take $c \sim 0.9$, to reasonably match with the latest CTEQ [31] parametrizations at these x and Q^2 values.

Observe that with the low- x dependence of (4.3) and the fact that (4.2) depends essentially on the squares of the gluon structure functions of each of the colliding hadrons, we obtain that our total cross-section increases linearly with s . Such a continued growth of σ of course violates general unitarity bounds and must eventually be halted, either from explicit higher twist corrections entering the gluon structure function [27], or/and from potentially

²In [13] when we considered the case that $G_{g/p}(x) \propto 1/x^{3/2}$, we mistakenly did not change normalizations of the gluon structure function when going from the case $G_{g/p}(x) \propto 1/x$. Using the normalization of (4.3) effectively reduces our rates for this case by one order of magnitude in Fig. 2 of [13].

novel low- x effects occurring in hadronic collisions [32]. At the present energies being considered however, the cross section is, as we will next see, exceptionally small. Hence it is unlikely unitarity constraints play much of a role and we expect all such corrections to be ignorable.

In Fig. 4 we plot the cross section at an upgraded Fermilab energy ($\sqrt{s} \sim 4$ TeV) and for the LHC ($\sqrt{s} \sim 14$ TeV). As a posthumous gesture, we also plot what the cross section would have been for the SSC ($\sqrt{s} \sim 40$ TeV). We used to obtain these plots: $\alpha_w \sim 1/30$, $\alpha_s \sim 0.1$, $m_W = 80.2$ GeV, and, as stated earlier, $c = 0.9$, $b = 4$ GeV $^{-2}$.

V. CONCLUSIONS

We have estimated the cross section for the exclusive diffractive production of an intermediate mass ($m_H < m_t$) Higgs particle at LHC and Fermilab upgrade energies using perturbative QCD methods. Due to the color-singlet nature of the hard event, we expect factorization to be applicable and the soft matrix elements entering the cross-section to be directly related to those entering exclusive, diffractive dijet events in ep collisions at HERA. Until such data is forthcoming, we have approximated these soft-matrix elements in terms of the gluon structure functions of the colliding hadrons in order to obtain a working estimate of the expected rates. We find that even at the most favorable conditions of the LHC (with a planned luminosity $\mathcal{L} = 1.7 \times 10^{34}$ (cm $^{-2}$ – sec $^{-1}$) [15]), the obtained cross section is at least several orders of magnitude below what one might consider a working level of usefulness.

A couple of factors might yet ameliorate somewhat these estimates. First, past experience [24,33,34] with exclusive processes in perturbative QCD indicates that the typical scale for evaluating the running coupling is generally significantly less than that of the hard scattering probe. Even with a generous reduction factor of two orders of magnitude, so that in our formulas, $\alpha_s(Q^2 = M_H^2) \rightarrow \alpha_s(Q^2 = (M_H/100)^2)$, this increases our estimate by at most by a factor of $(2)^4 = 16$. A second enhancement factor not unreasonable to expect comes from the experience with inclusive hard scattering collisions in which a K -factor type of correction

enters proton–proton vs. lepton–proton collisions. Guessing a typical value for $K \approx 2$, which should now however enter in the *amplitude* (Fig. 2), this would then lead to another factor of 4 or so increase in our rate. We thus find that altogether somewhere between one and two orders of magnitude enhancement above the rates depicted in Fig. 4 might not be unreasonable to expect. Unfortunately, even with such a total enhancement factor added, this still fails to bring up the magnitude of the cross section to what could be called experimentally useful levels (for the lightest Higgs masses in Fig. 4 these enhancements would correspond to a possible total of just a few such events per year at the LHC). Thus, despite the potential cleanness of the experimental signal, exclusive diffractive production does not appear to provide a viable channel for the detection of a standard model Higgs particle.

While hard double–diffractive scattering does not thus appear to be a feasible mechanism for probing new fundamental physics (i.e. Higgs discovery) we still believe the mechanism to be interesting in its own right for understanding the parton structure of the “pomeron” and addressing issues of factorization. We thus emphasize the importance of the experimental search for dijet double–diffractive events, a theoretical study of which is now being pursued to estimate expected yields at presently operating hadronic colliders, as well as those anticipated in the not too distant future.

Acknowledgements: We thank M. Banerjee, W. Broniowski, and M. Sher for their input. One of us (JM) would also like to thank Rebecca Celia for her many spirited discussions. This work was supported in part by the U.S. Department of Energy, under grant No. DE–FG02–93ER–40762.

REFERENCES

- [1] UA8 Collaboration, Phys. Lett. **B297**, 417 (1992).
- [2] ZEUS Collaboration (M. Derrick et al.), Phys. Lett. **B315**, 481 (1993); and “Observation of jet production in deep inelastic scattering with a large rapidity gap at HERA”, DESY preprint 94-063.
- [3] A. Schäfer, A. Nachtmann and R. Schöpf, Phys. Lett. **B249**, 331 (1990).
- [4] B. Müller and A.J. Schramm, Nucl. Phys. **A523**, 677 (1991).
- [5] A. Białas and P.V. Landshoff, Phys. Lett. **B256**, 540 (1991).
- [6] J. D. Bjorken, Phys. Rev. **D47**, 101 (1993).
- [7] J. Gunion, H. Haber, G. Kane, and S. Dawson, *The Higgs Hunter’s Guide* (Addison-Wesley, Menlo Park, CA 1991).
- [8] V. Barger and R. J. N. Phillips, “Collider Physics 1993”, University of Wisconsin preprint MAD/PH/780 (1993).
- [9] CDF collaboration, “Evidence for Top Quark Production in $\bar{p}p$ Collisions at $\sqrt{s} = 1.8$ TeV”, FNAL preprint FERMILAB-PUB-94/097-E (1994).
- [10] J.C. Collins, L. Frankfurt and M. Strikman, Phys. Lett. **B307**, 161 (1993).
- [11] A. Berera and D.E. Soper, “Diffractive jet production in a simple model with applications to HERA”, University of Oregon preprint OITS 536, AZPH-TH/94-02 (1994).
- [12] J. C. Collins, D. E. Soper and G. Sterman, Nucl. Phys. **B261**, 104 (1985) and **B308** 833, (1988); G. Bodwin, Phys. Rev. **D31**, 2616 (1985) and **D34**, 3932 (1986); J. C. Collins, D. E. Soper, and G. Sterman, in “Perturbative QCD” (A. H. Mueller, ed.) (World Scientific, Singapore, 1989).
- [13] H.J. Lu and J. Milana, Phys. Lett. **B313**, 234 (1993).

- [14] J. C. Collins, J. Huston, J. Pumplin, H. Weerts, and J. J. Whitmore, “Measuring Parton Densities in the Pomeron”, Michigan State and Penn State University preprint CTEQ/PUB/02, PSU/TH/136 (1994).
- [15] Particle Data Group (K. Hikasa *et al.*), Phys. Rev. **D45** I.1 (1992).
- [16] D0 collaboration, Phys. Rev. Lett. **72**, 2138 (1994).
- [17] G. Coignet, Proc. of the Symposium on Lepton and Photon Interactions, (Editors P. Drell and D. Rubin, Ithaca NY, 1993).
- [18] E. Papageorgiu, Phys. Rev. **D40**, 92 (1989); M. Drees, J. Ellis, and D. Zeppenfeld, Phys. Lett. **B223**, 454 (1989); M. Grabiak, B. Müller, W. Greiner, B. Soff, and P. Kock, J. Phys. **G15**, L25 (1989); R. N. Cahn and J. D. Jackson, Phys. Rev. **D42**, 3691 (1990); J. Norbury, Phys. Rev. **D42**, 3696 (1990); B. Müller and A. J. Schramm Phys. Rev. **D42**, 3699 (1990).
- [19] M. G. Ryskin, Z. Phys. **C57**, 89 (1993).
- [20] S.J. Brodsky, L. Frankfurt, J.F. Gunion, A.H. Mueller and M. Strikman, “Diffractive Leptoproduction of Vector Mesons in QCD”, SLAC preprint SLAC-PUB-6412 (1994).
- [21] S. Dawson and R. Kauffman, Phys. Rev. **D49**, 2298 (1994).
- [22] F. Wilczek, Phys. Rev. Lett. **39**, 1304 (1977); T. Rizzo, Phys. Rev. **D22**, 178 (1980).
- [23] S. J. Brodsky and G. P. Lepage, Phys. Rev. **D22**, 2157 (1980).
- [24] S. J. Brodsky and G. P. Lepage, in “Perturbative QCD” (A. H. Mueller, ed.) (World Scientific, Singapore, 1989).
- [25] C. E. Carlson and J. Milana, Phys. Rev. **D44**, 1377 (1991).
- [26] A. Donnachie and P. V. Landshoff, Phys. Lett. **B285**, 172 (1992).
- [27] L. V. Gribov, E. M. Levin and M. G. Ryskin, Phys. Rep. **100**, 1, (1983).

- [28] J. P. Ralston, Phys. Lett. B**172** 430, (1986).
- [29] H1 Collaboration, Nucl. Phys. B**407**, 515 (1993)
- [30] ZEUS Collaboration, Phys. Lett. B**316**, 412 (1993).
- [31] J. Botts, et al., Phys. Lett. B**304**, 159 (1993).
- [32] J. Milana, Phys. Rev. D**34**, 761 (1986).
- [33] V. L. Chernyak and A. R. Zhitnitsky, Phys. Rep. **112**, 173 (1984).
- [34] P. Stoler, Phys. Rep. **226**, 103 (1993).

FIG. 1. Effective gluon-Higgs coupling vertices induced by a heavy top-quark loop.

FIG. 2. Mechanism for hard-diffractive production of Higgs particle. The dominant contribution comes from the subprocess where the Higgs particle is produced through the hard diffraction of two parton-gluons. p_1, p_2 are the initial proton momenta, and p'_1, p'_2 are the corresponding final momenta.

FIG. 3. Feynman diagrams for the calculation of the hard scattering amplitude, representing respectively the (a) s -channel (7 diagrams), (b) u -channel (7 diagrams), and (c) four-gluon-vertex (5 diagrams) exchange. There is no t -channel color-singlet exchange. The Higgs line can be attached to any gluon-line, three-gluon vertex, or four-gluon vertex. The effective ggH , $gggH$ and $ggggH$ interaction vertices are given in the text.

FIG. 4. Cross section for the exclusive production of Higgs at various hadron colliders (Fermilab upgrade and LHC). The SSC case has been included solely for the melancholy.

$$\begin{aligned}
 i G_{\lambda\mu}^{ab}(\mathbf{k}_1, \mathbf{k}_2) &= \begin{array}{c} \text{H} \\ | \\ \lambda a \text{---} \text{---} \text{---} \text{---} \mu b \\ | \quad | \\ \mathbf{k}_1 \quad \mathbf{k}_2 \end{array} = \begin{array}{c} | \\ \text{---} \text{---} \text{---} \text{---} \\ | \end{array} \\
 &\quad + \text{permutation} \\
 \\
 i G_{\lambda\mu\nu}^{abc}(\mathbf{k}_1, \mathbf{k}_2, \mathbf{k}_3) &= \begin{array}{c} \text{H} \\ | \\ \lambda a \text{---} \text{---} \text{---} \text{---} \nu c \\ | \quad | \quad | \\ \mathbf{k}_1 \quad \mathbf{k}_2 \quad \mathbf{k}_3 \\ | \\ \mu b \end{array} = \begin{array}{c} | \\ \text{---} \text{---} \text{---} \text{---} \\ | \end{array} \\
 &\quad + \text{permutations} \\
 \\
 i G_{\lambda\mu\nu\sigma}^{abcd} &= \begin{array}{c} \text{H} \\ | \\ \lambda a \text{---} \text{---} \text{---} \text{---} \sigma d \\ | \quad | \quad | \\ \mu b \quad \nu c \end{array} = \begin{array}{c} | \\ \text{---} \text{---} \text{---} \text{---} \\ | \end{array} \\
 &\quad + \text{permutations}
 \end{aligned}$$

Fig. 1

This figure "fig1-1.png" is available in "png" format from:

<http://arxiv.org/ps/hep-ph/9407206v4>

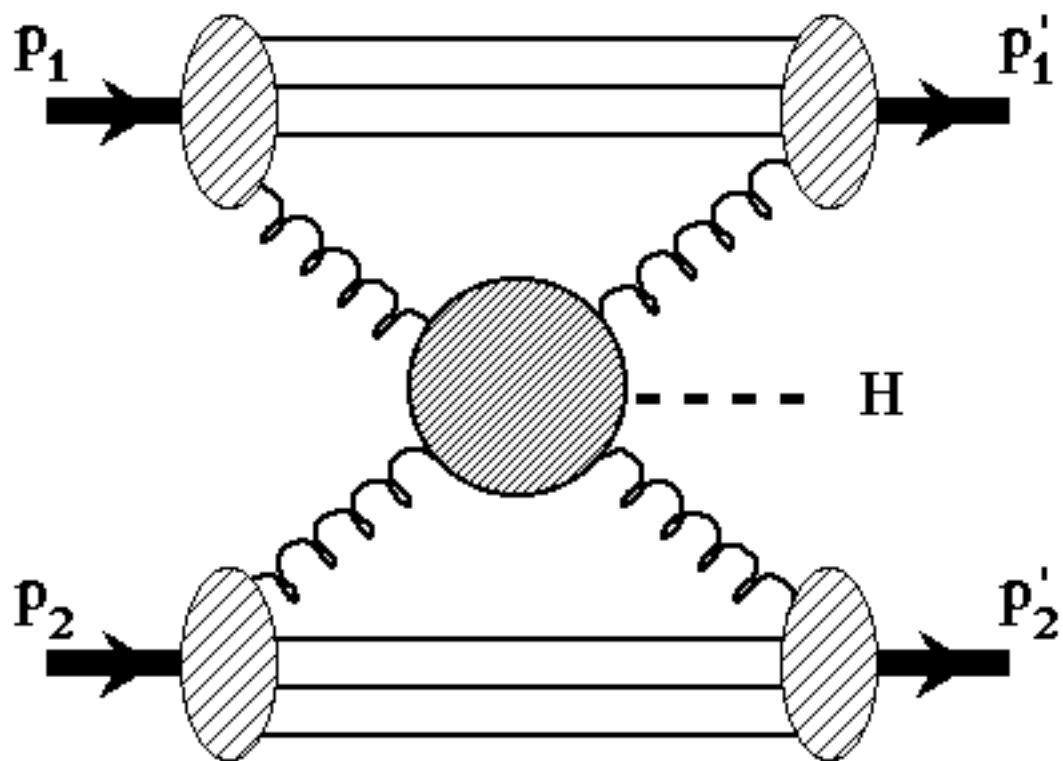


Fig. 2

This figure "fig1-2.png" is available in "png" format from:

<http://arxiv.org/ps/hep-ph/9407206v4>

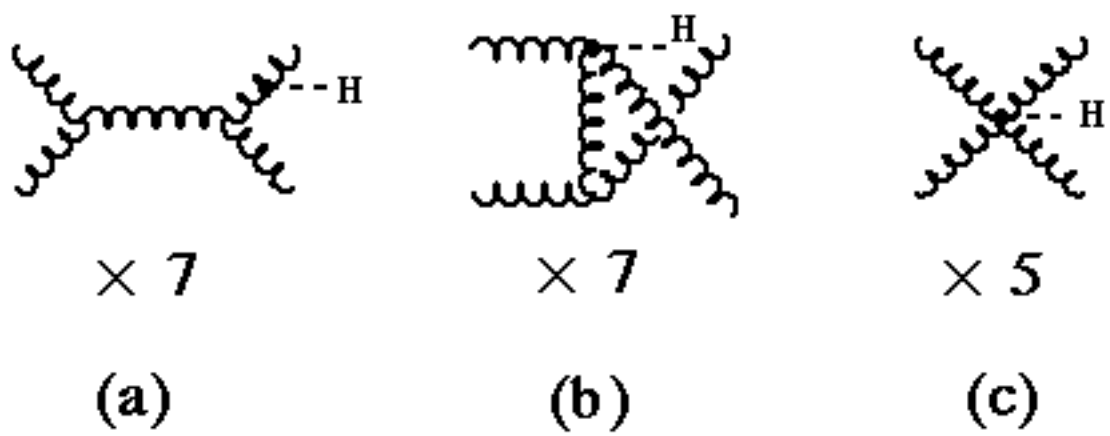


Fig. 3

This figure "fig1-3.png" is available in "png" format from:

<http://arxiv.org/ps/hep-ph/9407206v4>

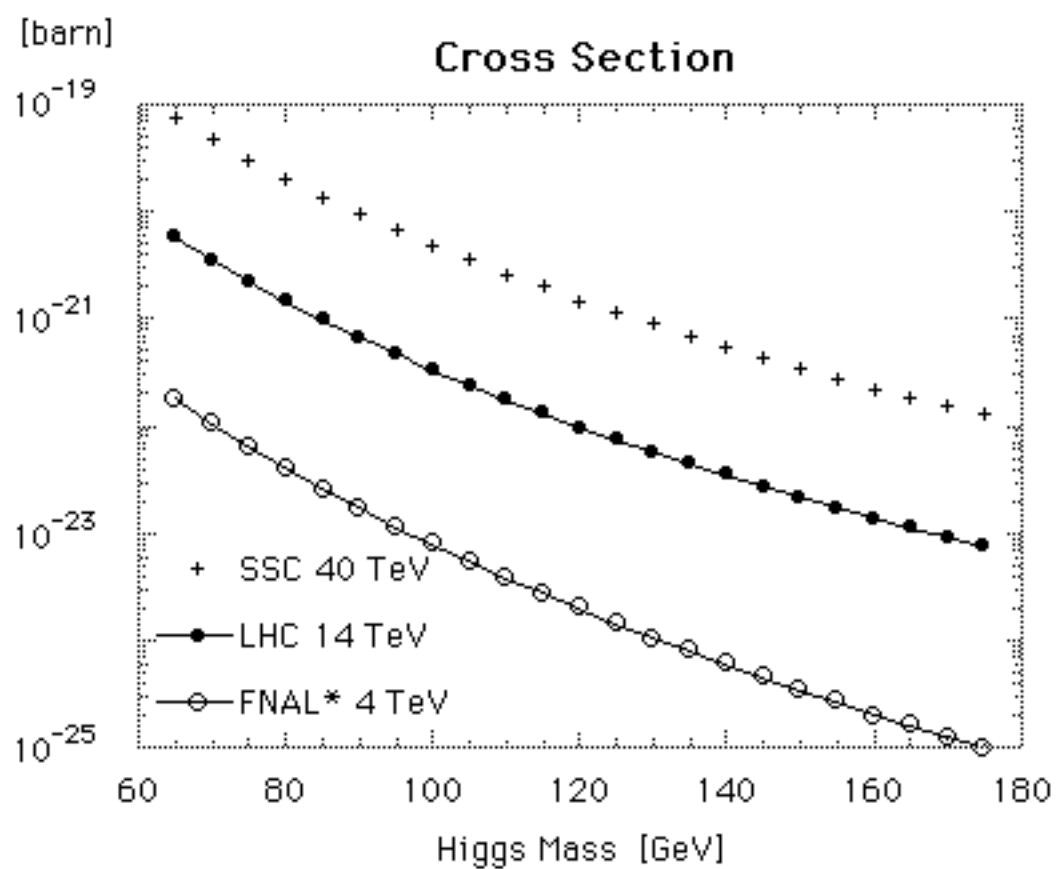


Fig. 4